Singapore Case Histories on Performance of Piles Subjected to Tunnelling-Induced Soil Movement

Cham Wee Meng, *Jacobs Services SEA Private Limited, Singapore; email: chamweemeng@yahoo.com.sg*

ABSTRACT: *In land scarce Singapore, the development of a comprehensive and efficient underground public transport system is the key to a sustainable transport system. This has resulted in many tunnels being built in densely urbanized areas and at close proximity to buildings and infrastructures. The tunnelling effects on these adjacent structures can be detrimental as problems such as pile settlement and passive loading on the piles could arise. The construction of large scale infrastructure projects such as Circle Line has opened up enormous scope for tunnelling and underground works in Singapore, which offers a great opportunity to study the response of piles to tunnelling. Two case histories are presented and involved the monitoring of 200 buildings located within the influence of tunneling along Circle Line (CCL) 3, 4 and 5. More than 3600 building settlement markers were analyzed and the resulting pile head settlements due to tunnelling were compared with surrounding ground surface movements. The results of the full-scale instrumented piles subjected to the effects of twin tunnel construction on adjacent groups of bored cast in-situ piles are also discussed.*

KEYWORDS: Tunnelling, Piles

SITE LOCATION: IJGCH-database.kmz (requires Google Earth)

INTRODUCTION

Tunnel construction is becoming popular for underground Metro Lines which are usually built in densely urbanized areas. The influence of such works near structures supported on piled foundations has increasingly become a source of major concern. Tunnelling effects can be detrimental to pile foundations as problems such as settlement of the ground and passive loading on the piles could arise.

The interaction between piled foundation and tunnel excavation is a complicated soil-structure-interaction problem and it is not well understood at present. Little information is available for design practice regarding the interaction between tunnels and piles. Land Transport Authority, Singapore, for example, specify that bored piles should not be constructed closer than 6m to existing tunnels. However, no limits are specified for the reverse problem.

Conventional design procedures for the assessment of the risk of tunnelling-induced damage on structures focused mainly on the assessment of the 'greenfield' surface settlement trough above the tunnel and its effect on the differential settlement to adjacent buildings. Although this may be appropriate for buildings supported on shallow foundations, this is unfortunately, in most cases, ignoring the piled foundation due to the complexities involved and the time investment required to perform accurate pile analysis. However, it should be noted that apart from the building assessment, the additional loading caused by subsurface soil movement could lead to excessive pile settlement or pile structural capacity being exceeded. Under-designed pile foundations will be reflected on the superstructure such as cracks on beam, column or wall and ultimately collapse, if the damage is substantial. As a result, expensive protective or mitigation works are usually proposed and this leads to high construction cost. Therefore, further studies would be required to develop a better understanding of the problem and contribute to an economic design.

At present, research on tunnelling induced pile response has not been extensive and very few field studies exist. This is because most structures were built before the tunnel alignments were planned. Therefore, the existing piles are not usually

Submitted: 12 December 2015; Published: 10 October 2016
Reference: Cham W.M. (2016). *Singapore Case Histories on Performance of Piles Subjected to Tunnelling-Induced Soil Movement*. International Journal of Geoengineering Case histories, http://casehistories.geoengineer.org, Vol.3, Issue 3, p.128-148. doi: 10.4417/IJGCH-03-03-01

instrumented and therefore it is not possible to assess or conduct an in-depth study on the behavior or the piles in response to the tunnelling works.

This paper intends to improve current knowledge for the pile response to tunnelling-induced ground movements by presenting the field results from full-scale instrumented piles and monitoring of 200 buildings located within the influence of tunneling along Circle Line (CCL) project in Singapore. More than 3600 building settlement markers are presented and analyzed.

CASE HISTORY 1 – FULL SCALE INSTRUMENTED PILES SUBJECTED TO TUNNELLING

The project involves the construction of twin bored tunnels from Marymount to Bartley station. This section of underground railway line was faced with many challenges as the alignment passes through heavily built-up areas consisting of residential buildings and infrastructures. The difficulties are associated with site constraints where tunnel alignment had to be constructed close to a large number of existing piled structures. Due to the envisaged mixed ground condition, Earth Pressure Balance Machines (EPBMs) were used.

The construction of these tunnels started in January 2006. The eastbound tunnel (TBM1) was driven first, followed by the westbound tunnel (TBM2) which was about 260 m to 480 m behind the eastbound tunnel (Both TBMs tunneling at west-east direction). The first crossing of the TBM1 below the five houses was in August 2006 and the second crossing of the TBM2 in December 2006.

The five terrace houses are situated within the tunnelling corridor as indicated in Figure 1. These two tunnels run parallel with lateral clearance of 2.5 m. As the piles are adversely affected by the tunnelling works, it was decided to acquire temporarily the five houses and rebuild them. In view of the uncertainty, some of the new piles were instrumented and several ground instruments were installed near the piles to monitor the effects of tunnelling.



Figure .1 Layout of the 5 houses and the tunnels' alignment.

Geology

The longitudinal section of the tunnel and the overlying geology is shown in Figure 2. The bedrock (GII and GIII) is generally varied in depth due to different degrees of weathering. In general, the subsoil comprises of the following strata along the tunnel alignment:

(a) Backfill (Fill);

(b) Peats, peaty and organic clays (Estuarine) of the Kallang Formation;

(c) Silty clays (Fluvial) of the Kallang Formation;

(d) Residual soils and completely weathered Bukit Timah Granite (GIV, GV);

(e) Moderately and slightly weathered Bukit Timah Granite (GII and GIII).

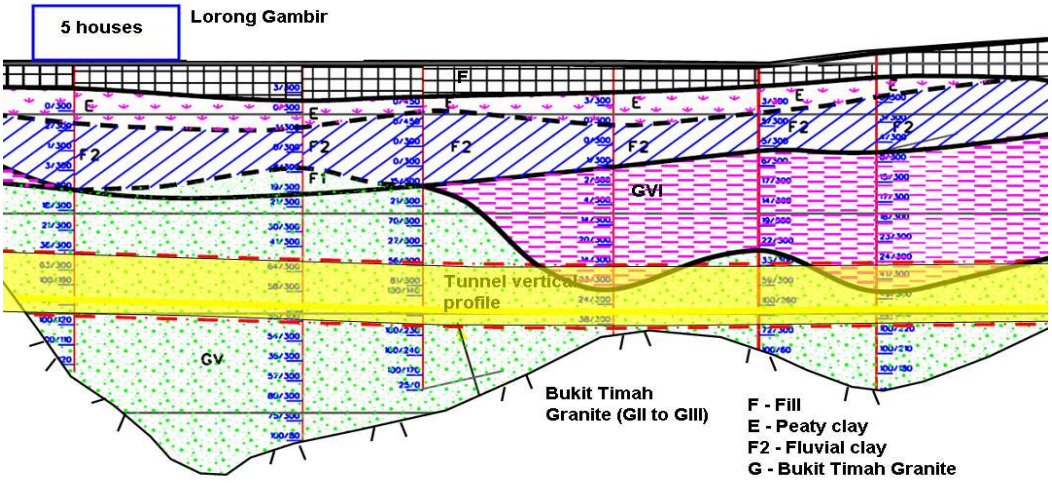


Figure 2. Longitudinal section of the tunnel and the overlying geology.

Details of Nearby 5 Lots of Terrace Houses

The structural scheme for the five terrace houses were reinforced concrete structures founded on piled-foundations. The reconstruction of the five houses started in July 2004 and was completed in January 2006. The piles were bored piles with diameter 600 mm, 800 mm and 1000 mm, ranging from 27 to 34 m long. The piling layout plan with reference to the tunnel alignment is shown in Figure 3. In this study, 5 piles were installed with strain gauges. They were single piles connected by a transfer beam at ground level. The details of the five instrumented piles are summarized in Table 1.

Table 1. Details of the as-built piles.

Pile number	Pile penetration Length (m)	Diameter (mm)	Lateral clearance between tunnel and piles (m)
BP1-E	27	600	1.0
BP1-H	31	600	1.65
BP1-G	31	600	1.65
BP2-E	33.4	800	1.0
BP1-A	27	600	4.1

As these piles were found within the Railway Protection Zone, they were de-bonded beyond the influence zone defined by 45 degree measured from the tunnel axis. The typical de-bonding length for such piles is shown in Figure 3.

De-bonding of the pile shaft has always been adopted as one of the construction methods to minimize the effect of negative skin friction. The proposed de-bonding system consisted of two layers of HDPE geomembrane and they were wrapped around the bored pile shaft (without bentonite) prior to concreting. This allows sliding to occur so as to mitigate the effect of negative skin friction. Theoretically, a smooth surface is frictionless and would not attract additional down-drag load on the pile due to soil movement.

With the de-bonding system, negative skin friction was assumed to be negligible and it was not considered in the design. The capacity of the pile was achieved by considering base resistance and shaft capacity from the non de-bonded section only.

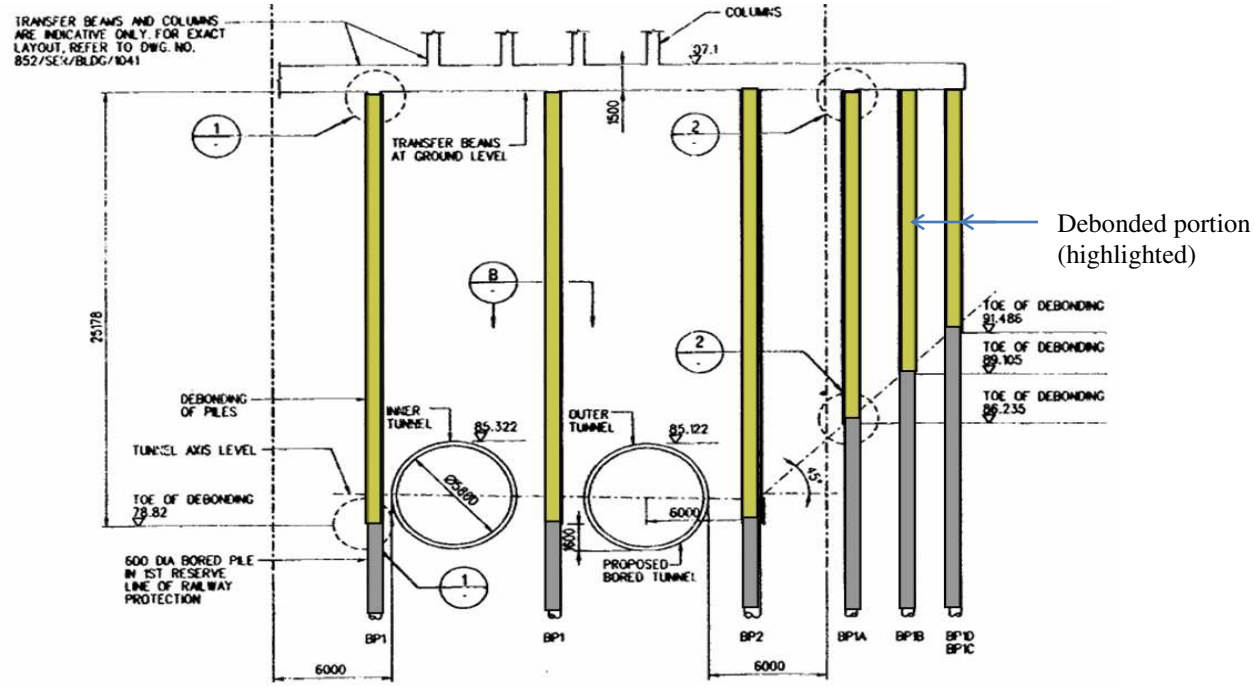


Figure 3. Schematic illustrating de-bonding length.

Earth Pressure Balance (EPBM) Tunnelling Machines

A detailed record of the TBMs' operation performance during construction of eastbound and westbound tunnels was examined during the periods when crossing beneath the five houses. Based upon case histories and results of extensive instrumentation observed in some tunnelling projects, face pressure and tail void grouting have been identified as the most important factors controlling ground movement.

The date of installation of each ring is given in Figure 4 for the two tunnels. The periods when the two tunnels are beneath the five houses are also indicated. The eastbound tunnel-drive crossed beneath the five houses approximately 4 months earlier than the westbound tunnel-drive.

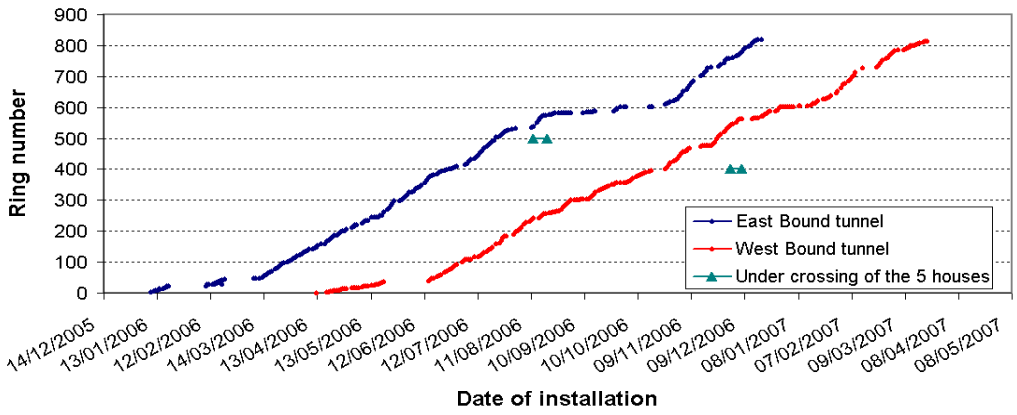


Figure 4. TBM schedule for eastbound and westbound tunnel.

Figure 5 shows the face pressure readings of the two TBMs. During tunnel operations, the tunnel face is supported by pressure built up in the excavation chamber. This face pressure is controlled by regulating the amount of discharge from the chamber. Monitoring of face pressure is essential as large pressure drop would result in surface settlement.

In view of the uncertainty of the tunnel-pile interaction that took place beneath the five houses, the face pressure was carefully controlled and monitored. This is evident as the face pressures fluctuate less during the period when the TBMs were beneath the houses. To support the overlying ground while tunnelling, adequate face pressure was maintained between 2.1 bars to 2.5 bars.

The measurements show that the mean face pressures for eastbound (2.1 bars) and westbound (2.2 bars) tunnels were almost similar during excavation beneath the five houses. However the control of face pressure in TBM2 was better as considerable scatter in the magnitude of the overall face pressure was observed in TBM1. For example prior to excavation of the eastbound tunnel beneath the 5 houses, it was observed that the face pressure changed abruptly from a maximum of 2.6 bars to as low as 1.8 bars. This was due to the replacement of cutter head as highlighted above. The difference in controlling the face pressure might explain the larger soil movements and heave encountered during excavation of eastbound tunnel.

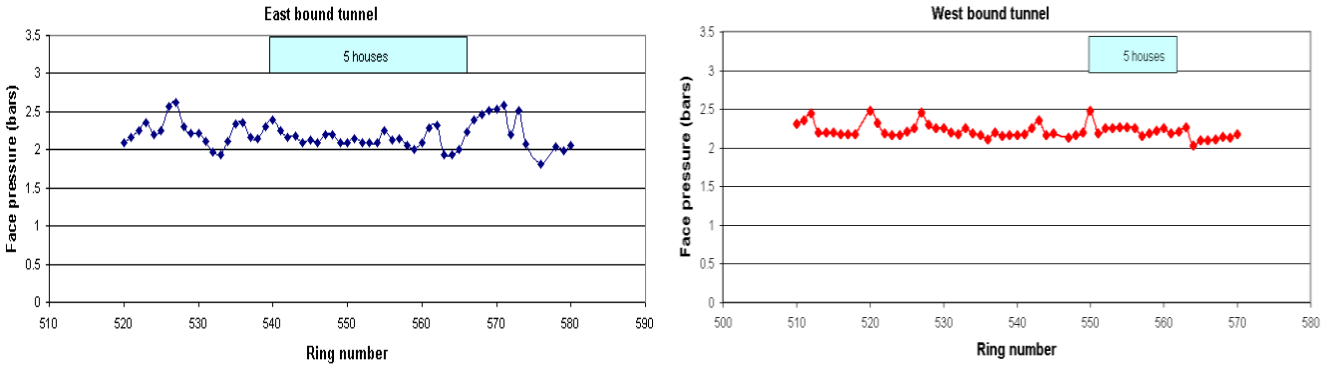


Figure 5 Application of face pressure.

Another important control of ground settlement is determined by the quality of tail void grouting. This is because as the shield is advanced forward, a tail void between the new lining and the surrounding soil is created. To prevent closing of the void, tail void grouting by injection is required. In addition, the grouting pressure should be high in order to ensure flow of grout and to prevent collapsing soil into the void. Figures 6 and 7 show the grouting pressures and volume of grout pumped during construction of the two tunnels. The grouting pressures beneath the five houses for eastbound and westbound TBMs were maintained at 3.4 bars and 2.8 bars respectively. The applied grout volume was about 4.0 m^3 to 4.5 m^3 per ring.

Generally, the mean grouting pressures for the eastbound tunnel are slightly higher than westbound. It was reported that ground over-cut occurred during excavation for the eastbound tunnel at ring number 576. To prevent large volume loss, 8.0m^3 of grout volume was injected. Similarly, an over-cut at ring number 564 of westbound took more than 8.0m^3 of grout volume to prevent soil settlement.

During the tunnel-drive beneath the five houses, G(V) material was consistently encountered. At this section, the average advancement rate is in the range of 20 to 24mm/min or about 6 rings per day.

The influences of these operating factors on the pile response are covered in monitoring results. A summary of the TBM operating factors when the two boring machines were beneath the houses are presented in Table 2 which shows the mean values.

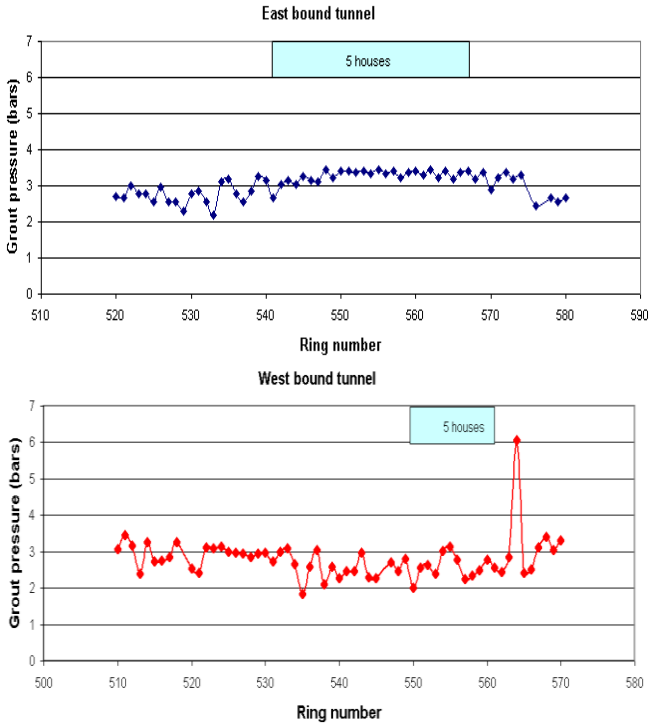


Figure 6. Application of grout pressure.

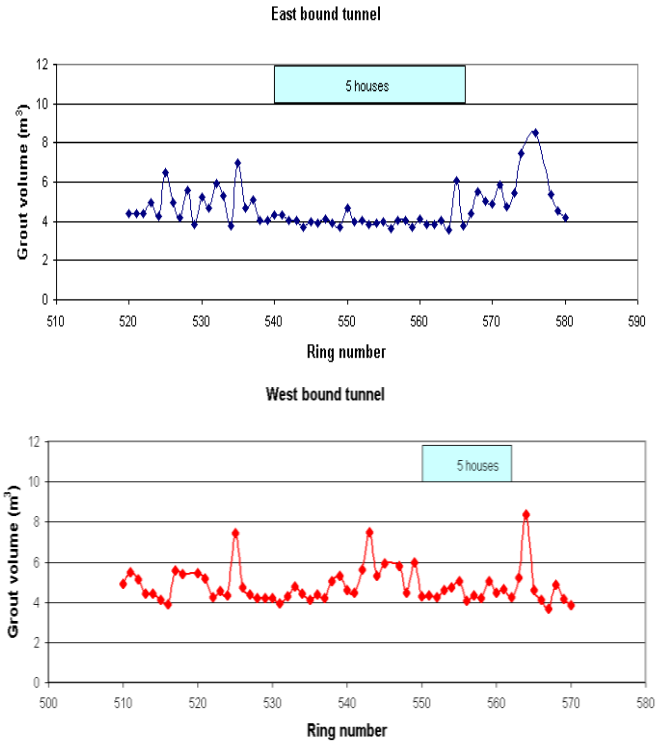


Figure 7. Application of grout volume.

Table 2. Summary of TBM performance.

TBM operation factors	Eastbound tunnel	Westbound tunnel
Face pressure (bar)	2.1	2.2
tail void grouting pressure (bar)	3.4	2.8
Grout volume (m^3)	4.0	4.5
Advancement rate (mm/min)	24	20
Thrust force (kN)	14000	15500
Cutter speed (RPM)	2.0	2.0
Screw conveyor speed (RPM)	6.0	5.0

Pile Instrumentation

Five piles were instrumented with vibrating wire strain gauges to monitor the axial force and bending moment along the pile. Figure 8 shows the layout of the five piles relative to the alignment of the twin tunnels. The levels at which the strain gauges were installed below ground were 2.5 m, 5.5 m, 19.3 m, 21.8 m, 25.3 m and 28.3 m as illustrated in Figure 9. They were mostly located between the tunnel crown and tunnel invert level. At each level, two pairs of strain gauges were placed at orthogonal positions such that one pair is perpendicular to the tunnel alignment. The measurement range was 2500 microstrain and the resolution was 1 microstrain.

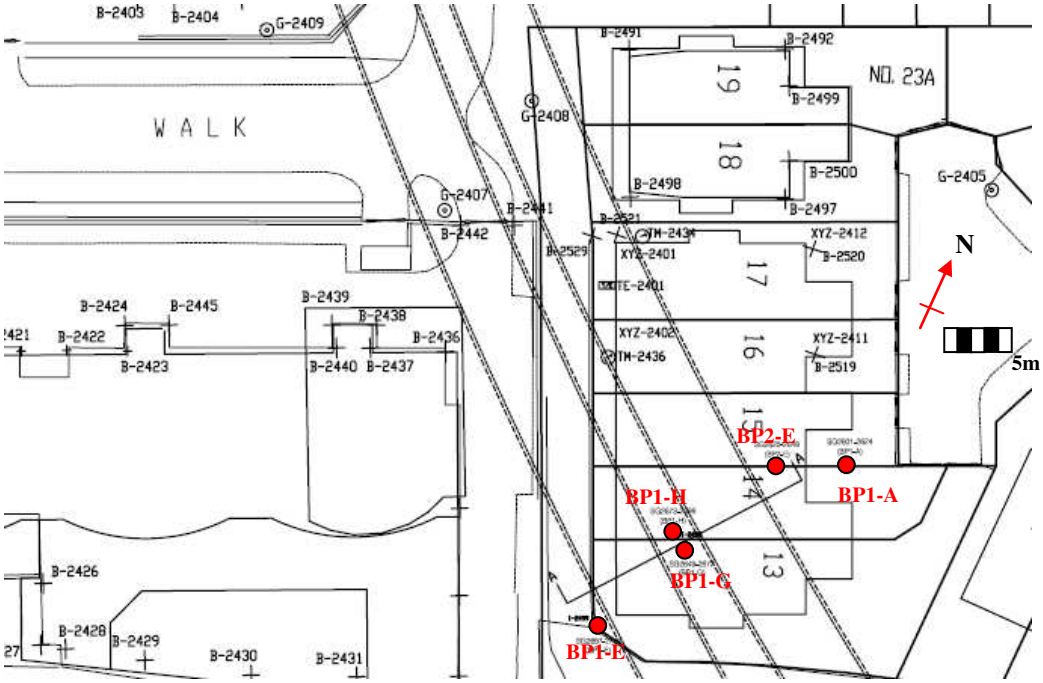


Figure 8. Layout of the five instrumented piles.

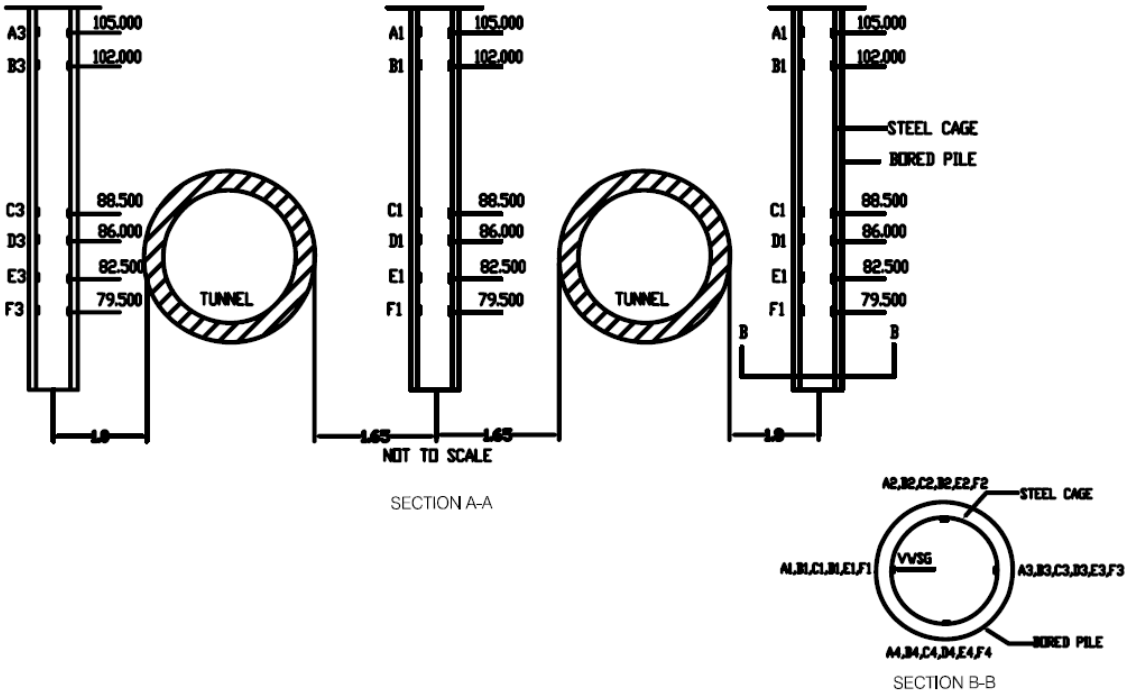


Figure 9. Six levels of strain gauges installed along the piles.

From the strain gauge measurements, the load distribution along the pile can be derived. Equation 1 is used to obtain the change in axial force by considering the average change in strains of the four strain gauges at each level.

$$\Delta N = E_{pile} A_{pile} \frac{\Delta\varepsilon_{x1} + \Delta\varepsilon_{x2} + \Delta\varepsilon_{x3} + \Delta\varepsilon_{x4}}{4} \quad (1)$$

Where ΔN = change in axial force (kN)
A_{pile} = cross section area of the pile (m^2)
E_{pile} = Young's modulus of pile (kN/m^2)
$\Delta\varepsilon_{1-4}$ = change in strain gauge readings at each level (dimensionless)

The Young's modulus of pile is derived based on ACI method using Equation 2. The Young's modulus was calculated as 25,000 MPa based on the pile's concrete grade of 35 N/mm^2. To account for the time-dependent creep strains that occur in each pile, the reduction of the pile's Young's modulus follow an exponential function shown in Equation 3 as proposed by Selemetas (2005). Over the course of two years since the completion of the piles, the value of the Young's modulus was down to approximately 60% of $E_{pile(max)}$. In this paper, 15,000 MPa was used to calculate the induced forces.

$$E_c = 151000\sqrt{f_c'}$$
$$f_c' = 0.8 f_{cu} \quad (2)$$

Where f_c' = characteristic compressive strength of concrete (kPa)
f_{cu} = concrete grade (kPa)

$$E_{pile} = E_{pile(\max)} t^{(-0.0819)} \quad (3)$$

Where t = the period since the completion of the pile (days)

The bending moments in longitudinal and transverse direction are derived based on Equations 4 and 5. The transverse bending moment is computed by considering the pair of strain gauges (ε_1 and ε_3) that are perpendicular to the tunnel alignment. For the longitudinal bending moment, strain gauges (ε_2 and ε_4) that are parallel to the tunnel alignment are used.

$$M_{xx} = E_{pile} I_{pile} \frac{(\varepsilon_{x1} - \varepsilon_{x2})}{d} \quad (4)$$

$$M_{yy} = E_{pile} I_{pile} \frac{(\varepsilon_{y1} - \varepsilon_{y2})}{d} \quad (5)$$

Where M_{xx} = Transverse bending moment (kN/m)
M_{yy} = Longitudinal bending moment (kN/m)
I_{pile} = Second moment area of pile (m^4)
E_{pile} = Young's modulus of pile (kN/m^2)
d = Distance between strain gauges (m)
ε_{1-4} = Strain gauges reading at each level (dimensionless)

Monitoring Results and Data Analysis

Induced Axial Load

A schematic diagram illustrating the positions of the piles relative to the tunnels is shown in Figure 10. The axial load was determined indirectly from measurements of strain. It is observed that additional down-drag forces were induced on the piles during the passage of the TBMs. This is a result of tunneling-induced soil settlement that generated negative skin friction on the pile shaft. The maximum down-drag force at each level was observed when the TBMs crossed the piles. As the TBMs moved beyond the piles, a slight reduction in down-drag force was observed in all piles. The tail void grouting is the cause of the reduction as high grouting pressure could result in soil heave and reduced stress in the piles. The findings are consistent with Pang (2006).

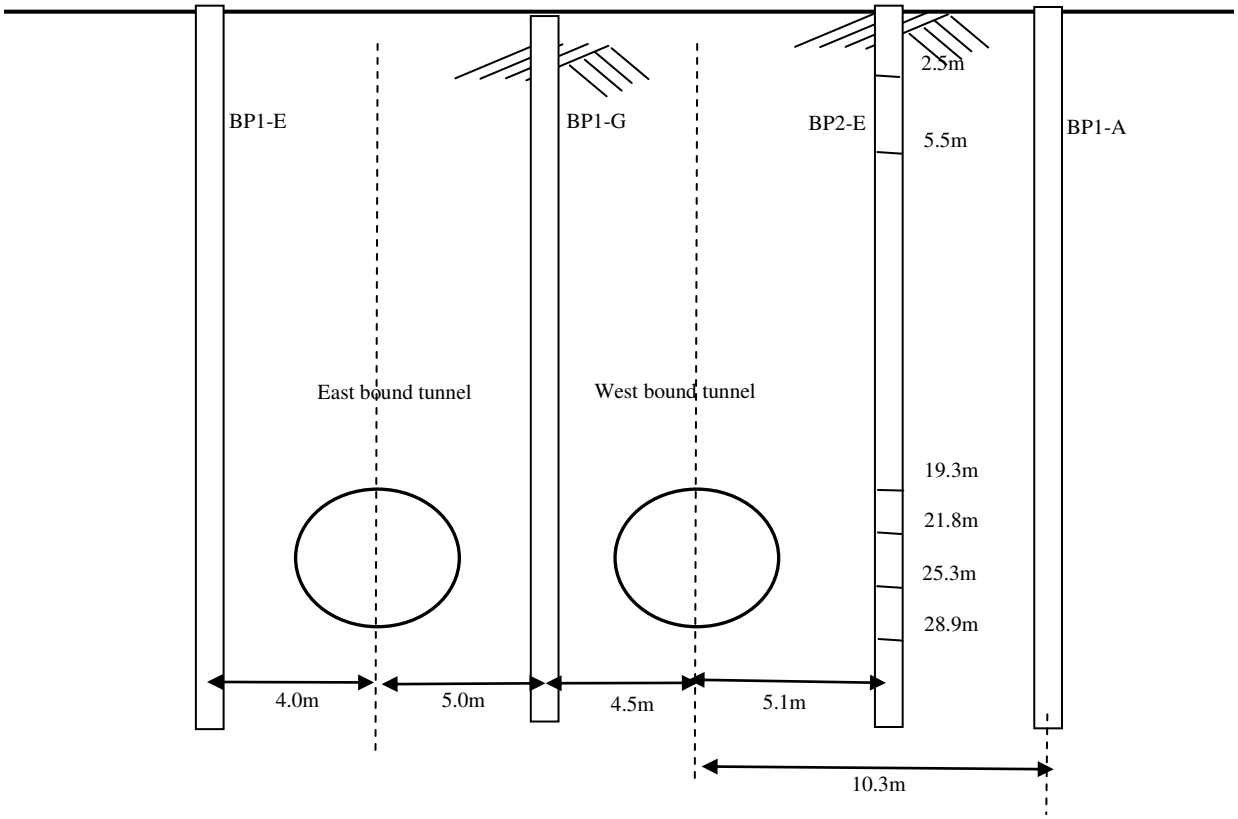


Figure 10. Illustration of pile positions relative to tunnels.

Figure 11 shows tunneling-induced axial force (i.e. in excess of their initial load) plotted against time at different depths of the piles. The axial load was determined indirectly from measurements of strain. Compressive forces are indicated by negative values. It is observed that additional compressive forces or down-drag force were induced on the piles during the passage of the TBMs. This is a result of tunneling-induced soil settlement that generated negative skin friction on the pile shaft. As observed in the figures, the maximum down-drag force at each level developed when the TBMs crossed beneath the piles. As the TBMs moved beyond the piles, a slight reduction in down-drag force was observed in all piles. This reduction is more noticeable in BP1-A which even generated tensile force near to the pile top during passage of eastbound tunnel. The tail void grouting is the cause of the reduction as high grouting pressure could result in soil heave and reduced stress in the piles. The findings are consistent with Pang (2006).

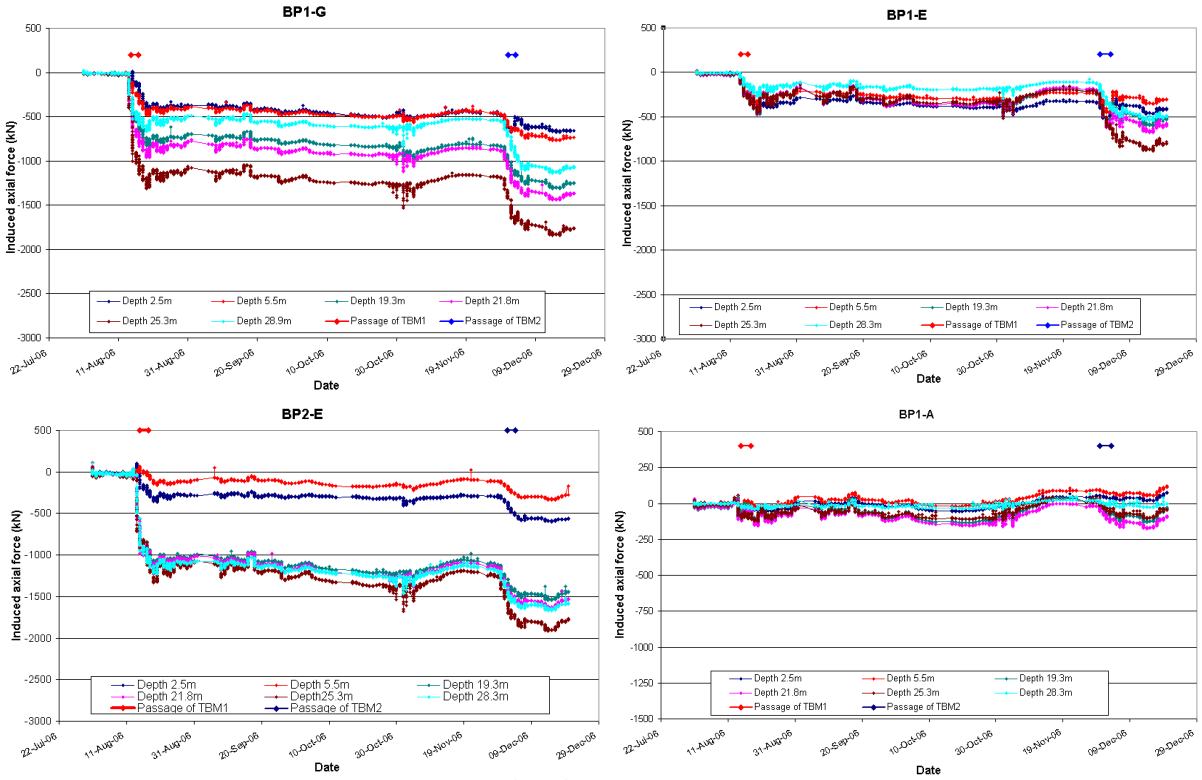


Figure 11. Induced axial force with time.

Figure 12 shows the distribution of induced axial force along BP1-G at various stages of eastbound tunnel excavation. Initially the pile only experienced minor increase in axial force when the approaching TBM was 15 m behind the pile. When the TBM was adjacent to the pile, slight increase in axial force (12.5% of the maximum recorded) was observed with its maximum slightly below tunnel axis level. As the tunnel advanced 10 m beyond the pile, a significant increase in axial force was registered due to the effect of tail void closure. At 20 m beyond the pile, the axial force increased slightly. The results agree reasonable well with Lee's (2005) three-dimensional coupled numerical analysis on pile response.

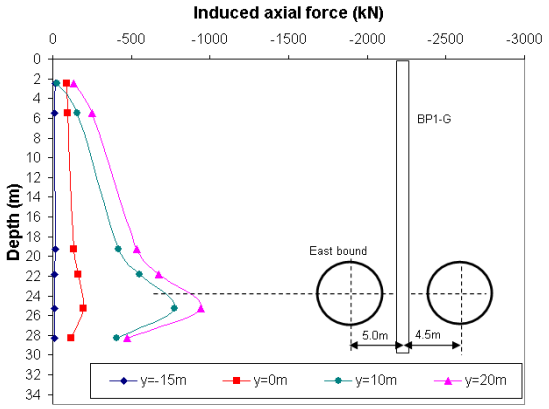


Figure 12. Distribution of induced axial force along BP1-G at various stages of excavation.

The final distribution of average induced axial force along the piles after the passage of TBM1 and TBM2 are shown in Figure 13. The analysis was carried out by resetting the change of strain to zero prior to the passage of the eastbound tunnel. Generally, the soil settlement due to tunnelling would induce negative skin friction on the pile shaft however this depends on the pile depth and offset relative to the tunnel. For this case, the pile tip is located below the tunnel axis level and the large soil settlement above the tunnel axis level would drag the pile down. This is evident from the observation in the figures as the down-drag forces are observed to increase with depth to tunnel axis level and decrease thereafter. The reduction is due to the development of shaft resistance (below the tunnel axis level) and base resistance to support the down-drag force.

Based on the as-built drawing, the cut-off level for the piles was at a distance of 1.5 m below ground level. With the first level strain gauges installed at 2.5 m b.g.l, it can be predicted that the down-drag forces measured near the pile head are negligible. Thus any load acting at this level should be approximately equal to the applied load. As non-zero value is observed near the head of each pile, the tunneling-induced pile settlements could have resulted in some re-distribution of structural loads on the piles after single and twin tunnel advancement. This is possible as the piles were connected by transfer beams and slab.

It can also be observed that a smaller increase in down-drag force acts on the upper 20 m of the pile shaft. This is an indication of the effectiveness of the de-bonding system. BP1-A experienced a negligible increase in induced axial forces after the twin tunnel advancement which accounts for only 7% of the pile structural capacity. BP1-G experienced a larger increase in induced forces as compared to BP1-E after the twin tunnel advancement. The difference in response could be due to different workmanship of the de-bonding system. Theoretically, a pile with a fully effective de-bonding system should experience zero down-drag force.

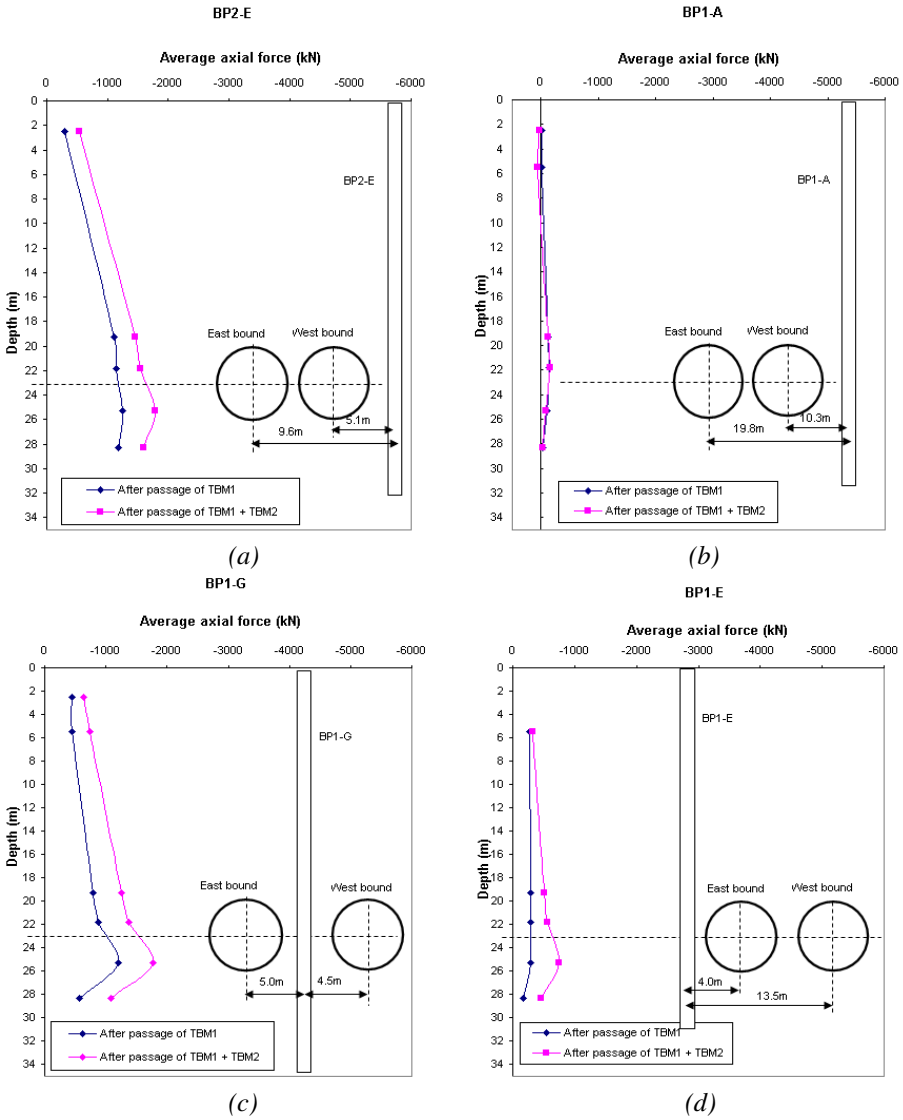


Figure 13. Distribution of induced axial force along a) BP2-E, b) BP1-A, c) BP1-G and d) BP1-E.

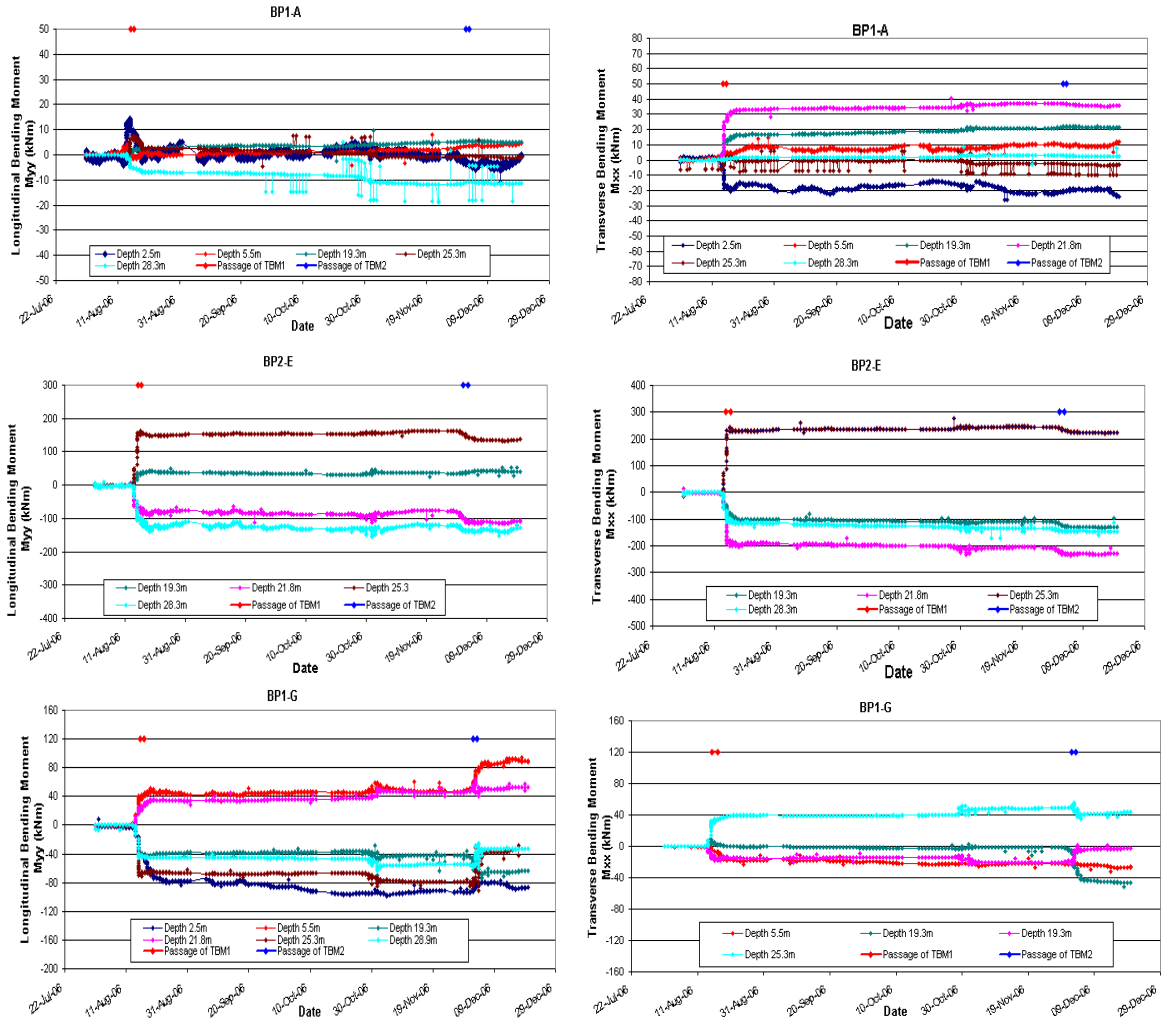
A summary of the maximum tunnelling-induced axial forces after single and twin tunnel advancement is shown in Table 3. The pile load test carried out at the site showed that the geotechnical capacity was higher than the structural capacity. Hence structural capacity was used as a pile design capacity. It can be seen that the maximum tunnelling-induced axial forces due to twin tunnel advancement ranged from 6% to 72% of the pile structural capacity.

Table 3. Summary of the maximum tunnelling-induced forces after single and twin tunnel advancement.

	Pile type	Max. induced forces (kN)	Pile structural capacity (kN)	Percentage (%)
After passage of TBM1	BP1-G	1195	2474	48
	BP1-E	288	2474	12
	BP2-E	1248	4398	28
	BP1-A	140	2474	6
After passage of TBM1+ TBM2	BP1-G	1768	2474	72
	BP1-E	753	2474	31
	BP2-E	1793	4398	41
	BP1-A	167	2474	7

Induced Bending Moments

Prior to tunnel excavation, the structural loads from the five houses induced negligible bending moments on the piles, which were designed as vertically loaded with no bending moment at the pile head. The induced bending moments due solely to tunnelling was determined by resetting the change of strain of strain gauges to zero prior to the passage of the eastbound tunnel. The longitudinal bending moment about an axis perpendicular to the tunnel alignment is denoted as M_{yy} and transverse bending moment about an axis parallel to it as M_{xx}.



(a) *(b)*

Figure 14. (a) Longitudinal and (b) transverse bending moment with time.

Figure 14a show the plots of induced bending moments in piles at different depths against time. Both longitudinal and transverse bending moments were measured. Generally, it is observed that the piles are subjected to additional bending moments of both positive and negative values after the passage of TBMs. Unlike axial force, no reduction in bending moment is observed after the passage of eastbound TBM.

Figure 14b shows the distribution of transverse and longitudinal bending moments along BP2-E at various stages of eastbound tunnel excavation. Initially the pile experienced negligible increase in bending moments in both directions when the approaching TBM was 15 m in front of the pile. When the TBM was adjacent to the pile, bending moments in both directions increased slightly with magnitude in the transverse direction larger than in the longitudinal direction. As the tunnel advanced 10 m beyond the pile, significant increases in bending moments were observed. At 20 m beyond the pile, no further increase in bending moments was observed.

The results agree reasonably well with the measured bending responses of a pile in pier 20 for C704 NEL (Pang, 2006) as included in Figure 15 for comparison. As can be seen, the bending moment profiles are similar although the maximum magnitudes occurred at slightly different levels.

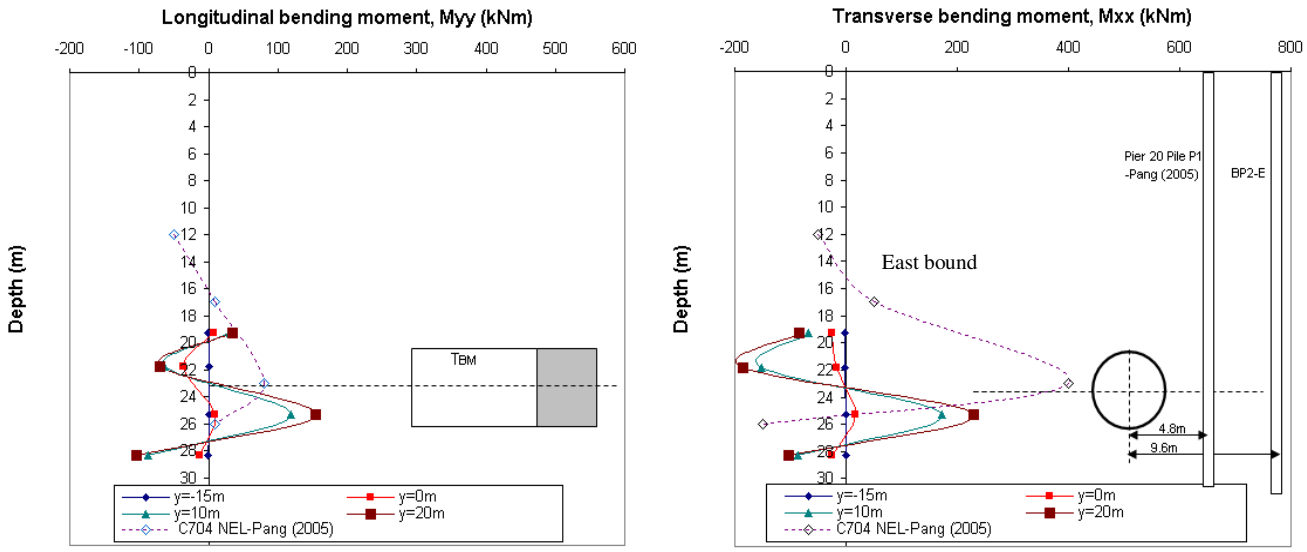


Figure 15. Distribution of bending moments along BP1-G at various stages of excavation.

The final distribution of average induced longitudinal and transverse bending moments along the piles after the passage of TBM1 and TBM2 are shown in Figure 16. Generally, the profiles indicate that the maximum transverse bending moments occurred near the tunnel axis level.

For BP2-E which is a 800 mm diameter pile, the maximum transverse bending moment recorded due to the passage of TBM1 is 221 kNm which is about 6 times higher than that of BP1-A. The large difference is a result of smaller offset between the eastbound tunnel and BP2-E. Furthermore, the larger diameter pile is stiffer and attracts more loads. The subsequent passage of TBM2 does not cause any significant change in the bending moment distribution. This could be a result of better operation control of the TBM and small volume loss.

BP1-G was subjected to bending in two directions owing to its location between the two tunnels. As a result, the induced bending moment profiles caused by eastbound and westbound tunnel excavations are opposite in directions. Hence the net increase in induced bending moment remains low. For the longitudinal response, the pile was seen to experience maximum bending moment at the pile head level. The result was consistent with the lateral soil movement, which shows large longitudinal movements at the upper part of the soil profile.

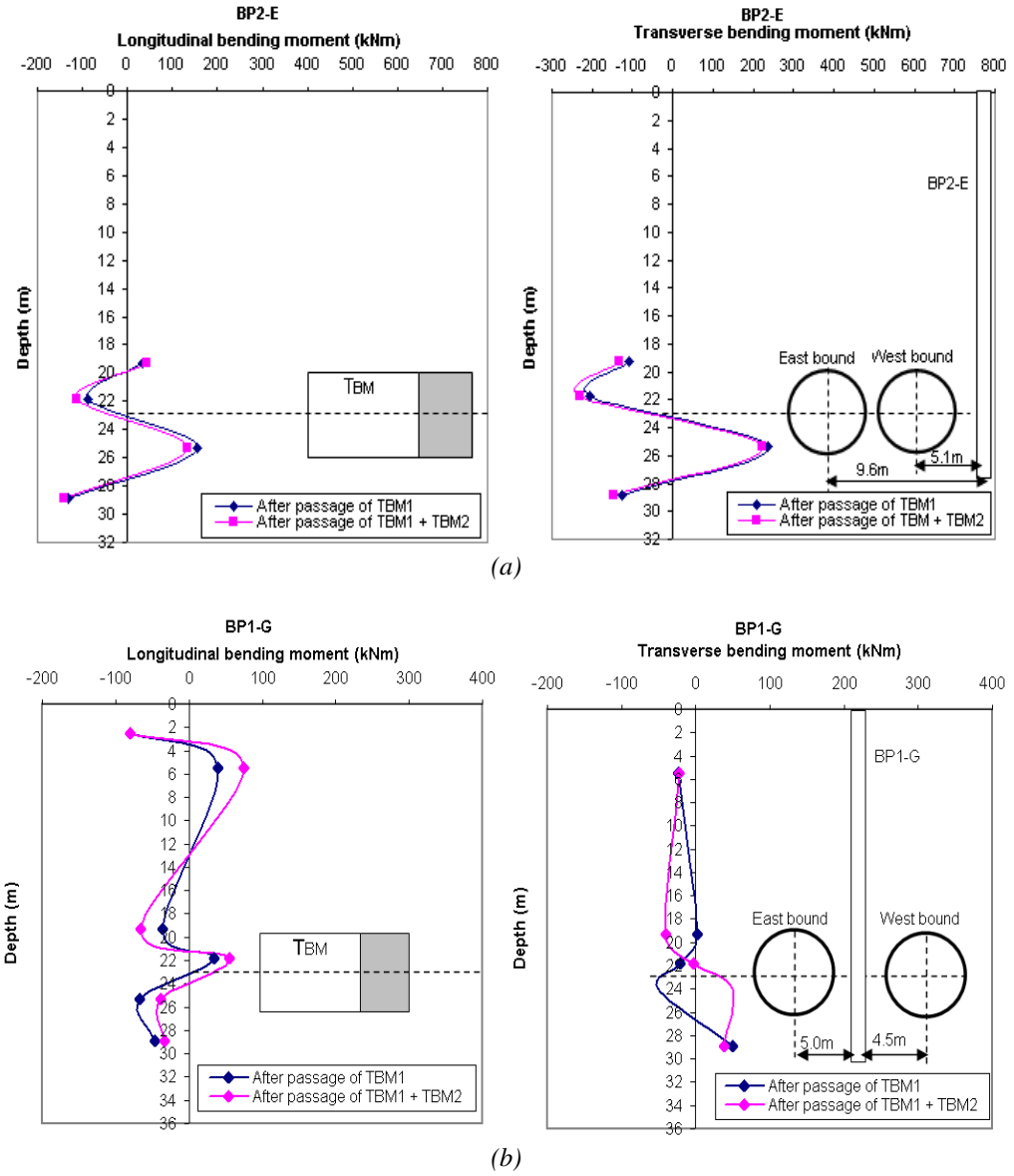


Figure 16. Longitudinal and transverse bending moment profiles along (a) BP2-E and (b)BP1-G.

The results also reveal that the transverse bending moments were found to be equal or larger than the longitudinal bending moments by up to 4.5 times. However this ratio is likely to depend on the magnitude of face pressure which would influence the pile response in the longitudinal direction. The findings are also consistent with Pang (2006) who reported that the longitudinal bending moment was smaller than the transverse bending moment by up to 5 times during a tunnel excavation in Singapore.

Effect of Lateral Distance to Pile Response

Figure 17 shows the pile forces plotted against pile depths for BP1-G and BP1-A. The bending moments and axial forces were measured due to the eastbound tunnel excavation at 0.5% volume loss. The results generally indicate that BP1-G has a higher pile response compared to BP1-A. This is because BP1-G is subjected to larger soil movement as the offset between tunnel centre-line and pile is smaller. This finding is in good agreement with Loganathan et al. (2001) that the distance effect is the main cause of the difference in pile response. Therefore based on the results, it would be safe to assume that the induced forces are negligible for horizontal offset beyond 3 times the tunnel diameter.

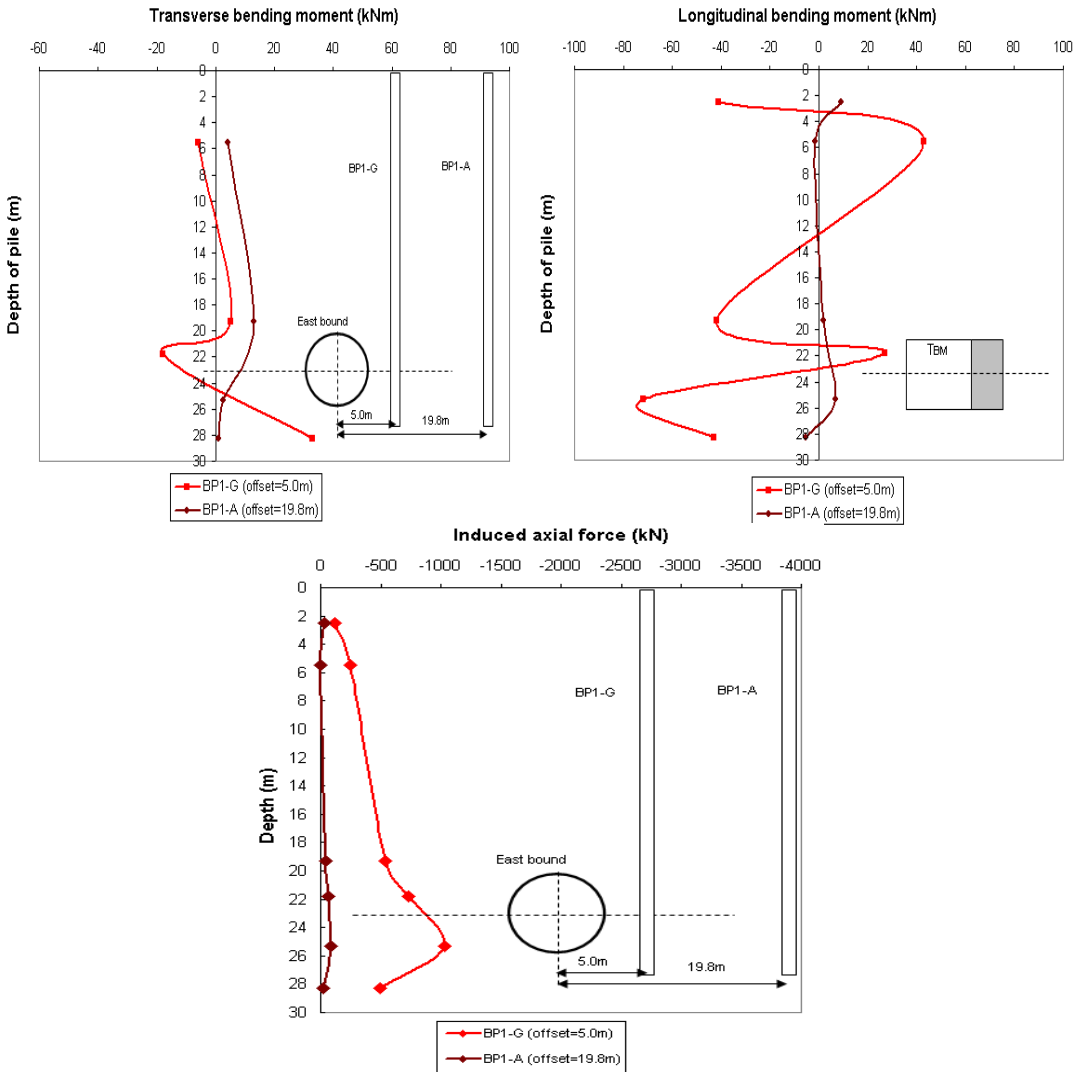


Figure 17. Influence of distance effect on induced bending moment and axial force.

Relationship between TBM Performance and Pile Response (Effect of Face Pressure)

The effect of tunnel face pressure on pile response was investigated by comparing the results of BP1_G subjected to eastbound and westbound tunnel excavation. For this case, the effect of lateral distance is negligible as the pile was located between the two tunnels.

Figure 18 shows the plot of depths against ratio of maximum induced forces by TBM2 over maximum induced forces by TBM1. Both induced axial forces and longitudinal bending moments at tunnel levels were considered. The average face pressures measured during excavation beneath the five houses were 2.1 bars and 2.25 bars for eastbound and westbound tunnels respectively. The results show that the ratio of induced forces is always less than 1 at the levels around the tunnel. This implies that higher face pressure induced lower magnitude axial forces and bending moments. This is because higher face pressure applied at the eastbound tunnel resulted in smaller ground volume loss and hence smaller pile responses.

In addition, it is observed that the ratio decreases with depth which means that the effect of face pressure on pile is more significant below tunnel axis level. The bending moments in the transverse direction were not significantly affected by the variation of face pressure and hence are not presented.

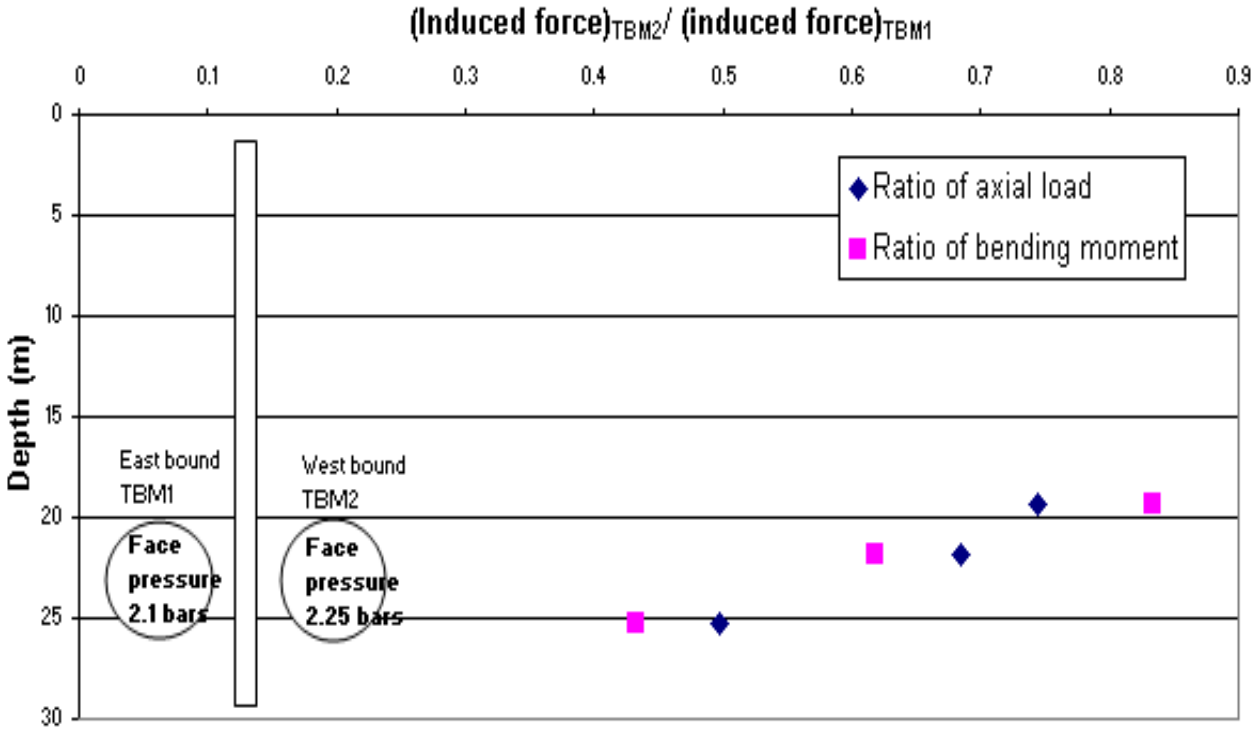


Figure 18. Effect of face pressure on pile response.

Conclusion

The results of five working piles instrumented with strain gauges are evaluated to check the response of piles during tunnelling. However it should be noted that the results of the monitoring data were limited to specific soil parameters, tunnel configurations, pile geometry and TBM performance. Nevertheless, these data provide valuable knowledge of some pile and ground responses to tunnelling. The following conclusions were made:

a) Maximum induced axial forces can be as high as 48% and 72% of the pile structural capacity after the advancement of single and twin tunnels respectively.
b) Maximum induced bending moments are measured near the tunnel level and their magnitude is small compared to their ultimate capacity
c) A significant zone of influence could be identified within a distance of 10 m ahead and 15 m behind the pile.
d) Maximum transverse bending moments were found to be equal or larger than the longitudinal bending moments by up to 4.5 times.
e) Induced forces are negligible for horizontal offset beyond 3 times the tunnel diameter.

CASE HISTORY 2 – SETTLEMENT OF PILED BUILDINGS AFFECTED BY TUNNELLING

The influence zones for the piled-building settlement were investigated using the data from CCL 3, 4 and 5. More than 200 buildings located within the influence of tunneling were studied and 3600 building settlement markers were presented and analyzed. They cover a wide range of building types, foundations, and soil conditions. The study discussed here is mainly due to the effects of tunnelling. The tunnelling methods included Earth Pressure Balance Machine and Slurry Tunnelling machines. Table 4 lists some of the affected buildings with details such as foundation type, distance between nearest pile and tunnel depth.

Table 4. Details of buildings and tunnels.

No.	Building/structures	Foundation details	Soil type in tunneling zone	Nearest distance to pile (m)	Tunnel depth (m)
1	2 storey detached houses at Jalan Harom Setangkai	RC piles. Depth unknown	Residual soil of Bukit Timah Granite	0 (outer)	26-28
2	25-storey flats at Kings Rd	Steel H-pile. 27m long	GV	6~48 (outer) 6~60 (inner)	21~25
3	5-storey Labrador Sub-station	800mm dia bored piles. 27m long	SV and SIII	3 (outer) 14 (inner)	14
4	7-storey Labrador Sub-station	700mm – 1250mm dia bored piles. 25m long	SV and SVI	1 (outer) 15 (inner)	13
5	2-storey shophouses at Pasir Panjang Road	Footing with bakau piles	SVI and Kallang Formation above	0 (outer) 5(inner)	17
6	3-storey Centre at West Coast Highway	150x150 RC piles/ 380 and 445 dia bored piles	SV/SVI	48 (outer) 64 (inner)	16
7	3-storey terrace houses at Pasir Panjang	RC piles	SIII/SV	40 (outer) 56 (inner)	16
8	3-storey semi detached houses at Pasir Panjang	Timber piles	SIII/SV	28 (outer) 44 (inner)	16
9	4-storey condominium at Pasir Panjang Rd	Bored piles	SVI	15 (outer) 60 (inner)	18
10	4-storey condominium at Pasir Panjang Rd	Timber piles	SVI	10 (outer) 59 (inner)	18
11	3-storey terrace house at South Buona Vista Rd	Piles	SV/SIV	33 (outer) 60 (inner)	19
12	3-storey shophouses at Pasir Panjang Rd	Piles	SV/SIV	33 (outer) 60 (inner)	19
13	3-storey terrace houses at West Ridge Walk	RC piles	SV/SIV	50 (outer) 69 (inner)	19
14	5-storey Currency House at Pasir Panjang Rd	700mm dia bored piles depth 30m	SVI/SIV	2 (outer) 13 (inner)	17
15	8-storey apartment at Pasir Panjang Rd	Piles	SIII	8 (outer) 21 (inner)	15
16	Electrical sub-station at Telok Blangah Rd	Piles	SIII	7 (outer) 0 (inner)	12
17	NTU Alumni	1.3m and 1.5m dia bored piles	SIII/SIV	0 (outer) 0 (inner)	34
18	12-sty high rise apartment at Belmont Rd	Bored piles 25m deep	G(VI)	2.5 (outer) 55 (inner)	12
19	2-sty Bungalow House at Belmont Rd	200x200 RC piles	G(VI)	9 (outer) 65 (inner)	20

Determination of Tunnelling Influence Zones

Figure 19 shows the measured building settlement plotted against lateral distance for different volume loss. As it is difficult to differentiate the settlements attributed to various tunnel drives near to each building, the data plotted in Figure 19 (and reported in this paper) are based on the building settlements induced by the first tunnel drive and before the influence zone of the second tunnel passed into the building. In general, the settlement of the piled-buildings decreased with increasing lateral distance from the tunnel centerline, and also increased with volume loss induced during tunnelling.

Another point to note is that buildings with large settlements have been omitted from this study, such as buildings above tunnelling under poor ground conditions with large volume losses. From the centrifuge studies, Jacobsz et al (2001) observed that some load re-distribution between pile shaft and pile end-bearing occurred when the volume loss increased. Specifically, skin friction first increased at the pile base before reducing as the end-bearing resistance increased. The load-carrying behaviour of the pile (and thus building settlement) would be different under normal conditions compared to high volume losses. Hence building settlement due to volume losses in excess of 3% were omitted in this study. It may be seen from Figure 19 that if volume loss is controlled to within 2%, the maximum building settlement would be 25 mm for buildings on piles, and less than 35 mm if the volume loss is 3%.

Figure 20 plots the normalized building settlement against the distance of the building from the tunnel normalized against the tunnel depth. By drawing envelopes to the normalized piled-building settlement data, it may be possible to categorise the data into three envelopes and estimate the piled-building settlement according to the tunnelling volume loss. In terms of influence zone, the pile settlement is found to be negligible at a horizontal distance of 1.5 times the tunnel depth (1.5*Z), when the volume loss is less than 1%, and increasing to 2*Z and 3.5*Z for volume losses that are up to 2% and 3% respectively. In terms of the maximum settlement, it was observed that the maximum piled-building settlements were found to be 0.05% and 0.1% of tunnel depth when the induced volume losses are 1% and 2% respectively.

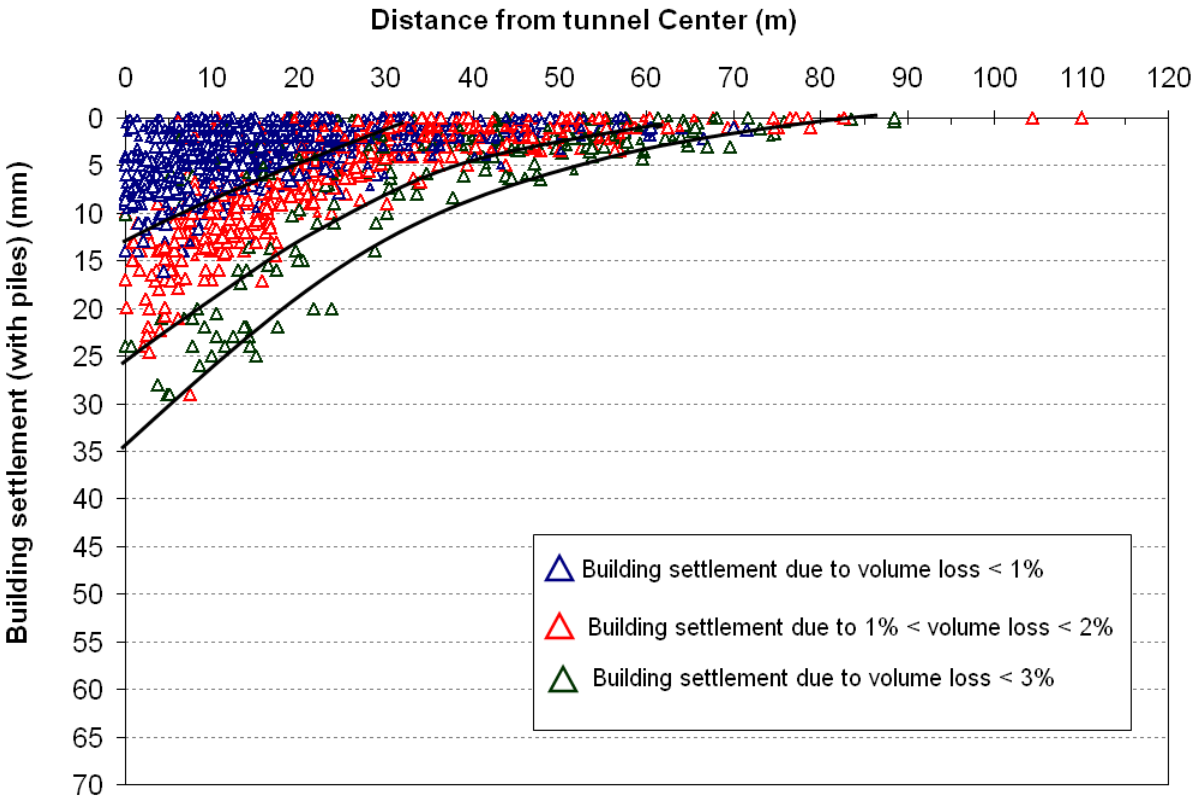


Figure 19. Tunnelling induced piled-building settlement.

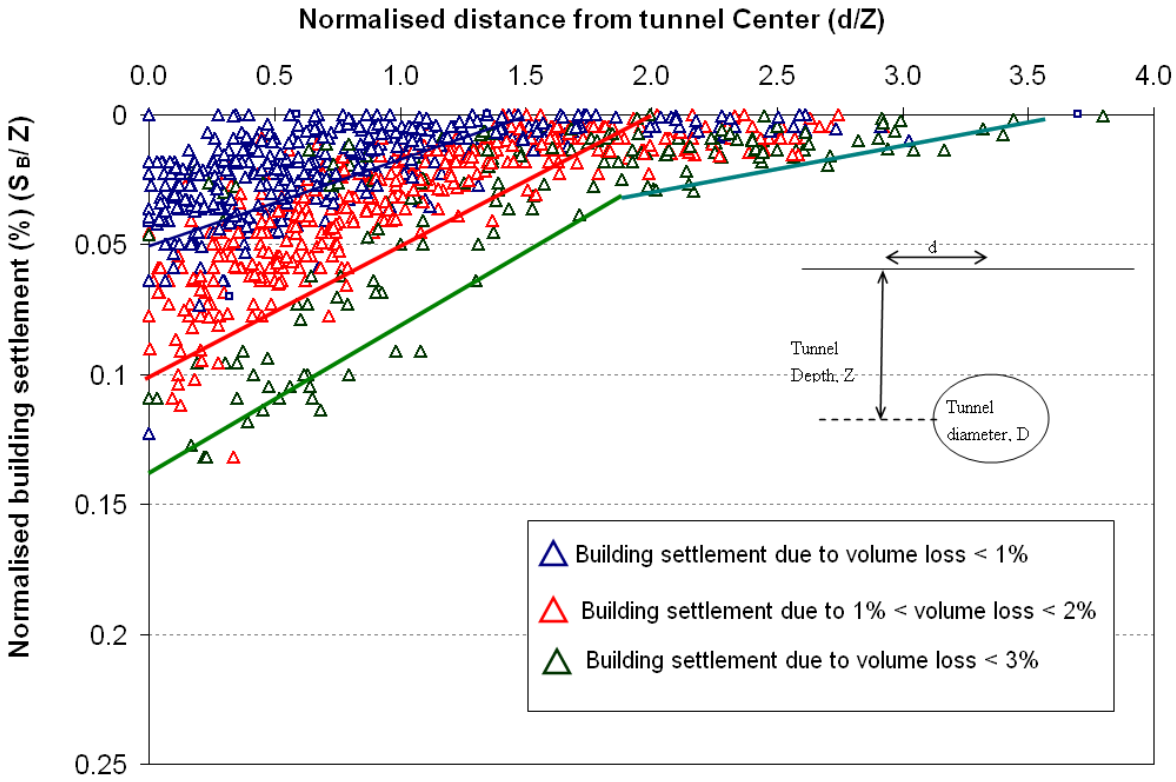


Figure 20. Normalized induced piled-building settlement.

Following the model by Selematas et al. (2005), a study was done to verify if the building settlements during the CCL works would follow the settlement zones identified by previous researchers, by comparing the measured piled-building settlements (S_B) with the measured surrounding ground settlements. A theoretical Gaussian function was fitted into the ground settlement arrays near each building, and the ground settlement coinciding with the building marker location (S_G) was estimated from the fitted Gaussian function. Figure 21 plots the ratio $(S_B)/(S_G)$ against the normalized distance of the building from the tunnel centerline, where it is possible to sub-divide the influence zones of tunnelling-induced movements onto a piled building.

For S_B/S_G ratio greater than unity, the building has settled more than the ground surface. Following on the work by Kaalberg et al. (2005), the zone where building has settled more than the ground surface can be approximately defined as a 30^o line drawn from the tunnel centre-line. This would coincide with the settlement data in Zone 1 of Figure 21. Defining the adjacent zone with an approximate 45^o line drawn from the tunnel centre-line, a Zone 2 can be drawn between d/Z of 0.75 and 1.2 as shown in Figure 21, and this coincided with the data points where the maximum S_B/S_G ratio is one. It is noted that there are many points in Zone 2 whose S_B/S_G ratio is less than one. This is due to the fact that the location of S_B relates to the building settlement marker, rather than the position of the pile toe which Kaalberg et al.'s (2005) model is based upon. For those buildings whose pile toes are below the 45^o line, then the S_B/S_G ratio would be expected to be less than one. Nevertheless, for buildings which are beyond Zone 2, where the building has settled less than the ground surface (i.e. S_B/S_G ratio less than 1), a Zone 3 can be defined at a distance of d/Z more than 1.2.

Although Figure 21 relates to building location rather than pile position, the influence zones are consistent with the earlier studies by Jacobsz et al. (2001), Selemetas et al. (2005), and Kaalberg et al. (2005), which relates to pile position. The zones defined using building position as shown in Figure 21 can be used as a guidance to derive the envelope of maximum S_B/S_G ratio, even if the exact pile toe position is not known. This would be useful in the design stage to allow planning for the tunnel alignment in proximity to adjacent pile buildings.

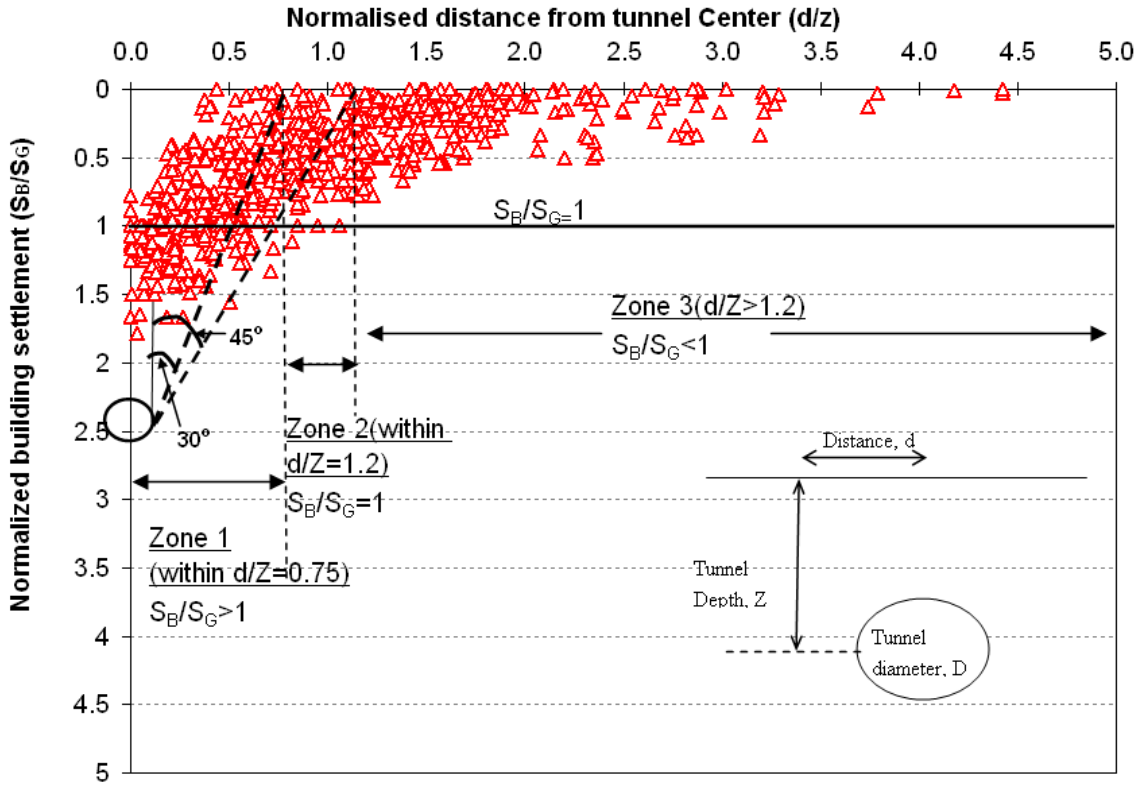


Figure 21. Influence zone of tunnelling.

Conclusion

The results of piled-building settlement caused by tunneling along Circle Line Stage 3, 4 and 5 are presented. Charts showing the envelopes of maximum normalized piled-building settlement are established for estimating the settlement of piled buildings.

Three zones of influence were identified in which pile settlements were correlated to surface ground settlements:

1. Buildings in **Zone 1** (i.e. distance within 0.75*Z from tunnel centerline) settled more than the ground surface settlement in the greenfield.
2. Buildings in **Zone 2** (i.e. distance between 0.75*Z and 1.2*Z from tunnel centerline) settled up to as much as the ground surface settlement in the greenfield.
3. Buildings in **Zone 3** (i.e. distance greater than 1.2*Z from tunnel centerline) settled less than the ground surface settlement in the greenfield.

The chart is developed based on the results of a large number of actual data in CCL projects. It is hoped that the presented chart can be a useful reference for engineers undertaking future building assessment in Singapore where accuracy of piled-building settlement profile is of great importance.

REFERENCES

Cham, W. M. (2007). "The response of piles to tunnelling." Degree of Master of Science (M.Sc) and Diploma of Imperial College (DIC), Imperial College, London.

Coutts, D. R. and Wang, J. (2000). "Monitoring of reinforced concrete piles under horizontal and vertical loads due to tunnelling." *Proc.,Tunnels and Underground Structures*, Balkema, Singapore, 541-546.

Jacobsz, S. W., Standing, J. R., Mair, R. J., Soga, K., Hagiwara, T. and Sugiyama, T. (2001). "Tunnelling effects on driven piles." *Proc. of Int. Conf. on Response of Buildings to Excavation-Induced Ground Movements*. Ciria, London, 337-348.

Kaalberg, F. J., Teunissen, E. A. H., van Tol, A. F. and Bosch, J. W. (2005). "Dutch research on the impact of shield tunnelling on pile foundations." *Proc., 5th International Symposium on Geotechnical Aspects of Underground Construction in Soft Ground*, CRC Press, Amsterdam, The Netherlands, 123-132.

Lee, G. T. K. and Ng., C. W. W. (2005). "Three-dimensional numerical simulation of tunnelling effects on an existing pile." *Proc., 5th International Symposium on Geotechnical Aspects of Underground Construction in Soft Ground*, CRC Press, Amsterdam, The Netherlands, 139-144.

Loganathan, N., Poulos, H. G. and Xu, K. J. (2001). "Ground and pile-group responses due to tunnelling," *Soils and Foundations J.*, 41(1), 57-67.

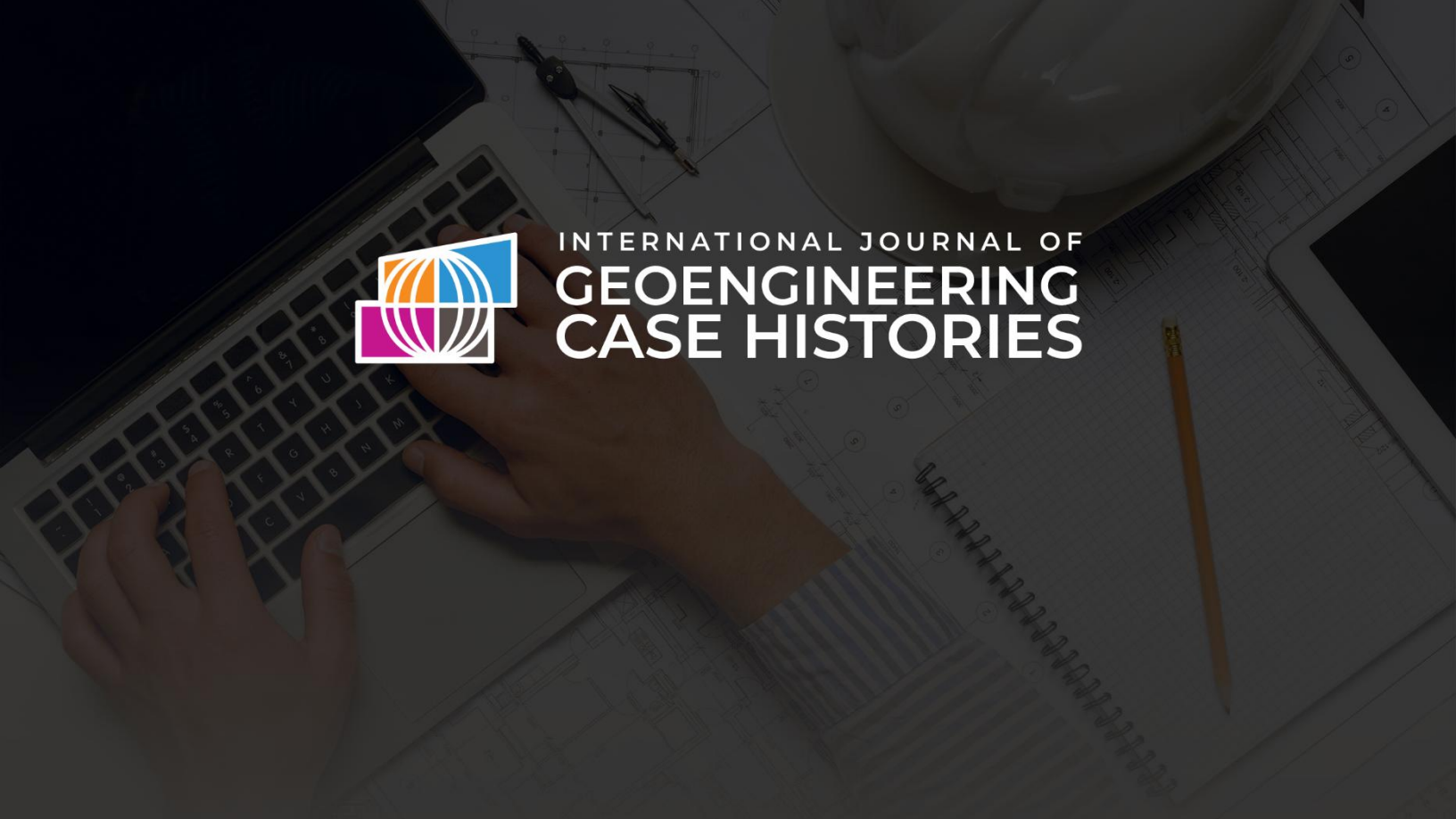
Mair, R. J. (2013). "Tunnelling and deep excavations: Ground movements and their effects." *Proc., 15th European Conference on Soil Mechanics and Geotechnical Engineering, Geotechnics of Hard Soils – Weak Rocks (Part 4)*, IOS Press, Athens, Greece, 39-70.

Pang, C. H. (2006). "The effects of tunnel construction on nearby piled foundation." PhD thesis, National University of Singapore, Singapore.

Selemetas, D. (2005). "The response of full-scale piles and piled structures to tunnelling." PhD thesis, Cambridge University, Cambridge.

Selemetas, D., Standing, J. R. and Mair, R. J. (2005). "The response of full-scale piles to tunnelling." *Proc., 5th International Symposium on Geotechnical Aspects of Underground Construction in Soft Ground*, CRC Press, Amsterdam, The Netherlands, 763-770.

Shirlaw, J. N., Richards, D. P., Ramond, P. and Longchamp, P. (2004). "Recent experience in automatic tail void grouting with soft ground tunnel boring machines." *Proc., 30th ITA-AITES World Tunnel Congress*, Elsevier, Singapore, 446-453.



INTERNATIONAL JOURNAL OF
GEOENGINEERING
CASE HISTORIES

The Journal's Open Access Mission is generously supported by the following Organizations:

dar
a Sidara company

Geosyntec consultants
engineers | scientists | innovators

CONETEC
MUD BAY DRILLING
LANKELMA
Geotech DRILLING

ENGEO
Expect Excellence

Access the content of the ĪSSMGE Īnternational Journal of Geoengineering Case Histories at:
www.geocasehistoriesjournal.org

Downloaded: Thursday, November 19 2026, 08:41:51 UTC